UNIVERSIDADE FEDERAL DE JUIZ DE FORA
CENTRO INTEGRADO DE SAÚDE
FACULDADE DE ODONTOLOGIA

Karolina Aparecida Castilho Fardim

QUANTIFICAÇÃO DE ARTEFATOS METÁLICOS PRODUZIDOS POR IMPLANTES DENTÁRIOS EM IMAGENS DE TOMOGRAFIA COMPUTADORIZADA DE FEIXE CÔNICO OBTIDAS COM DIFERENTES PROTOCOLOS DE AQUISIÇÃO

Juiz de Fora
2018

KAROLINA APARECIDA CASTILHO FARDIM

QUANTIFICAÇÃO DE ARTEFATOS METÁLICOS PRODUZIDOS POR IMPLANTES DENTÁRIOS EM IMAGENS DE TOMOGRAFIA COMPUTADORIZADA DE FEIXE CÔNICO OBTIDAS COM DIFERENTES PROTOCOLOS DE AQUISIÇÃO

Exame de Defesa apresentado ao Programa de Pós-Graduação em Clínica Odontológica, da Faculdade de Odontologia da Universidade Federal de Juiz de Fora, como requisito para obtenção do título de Mestre. Área de concentração em Clínica Odontológica.

Orientadora: Profa. Dra. Karina Lopes Devito

Juiz de Fora

2018

KAROLINA APARECIDA CASTILHO FARDIM

QUANTIFICAÇÃO DE ARTEFATOS METÁLICOS PRODUZIDOS POR IMPLANTES DENTÁRIOS EM IMAGENS DE TOMOGRAFIA COMPUTADORIZADA DE FEIXE CÔNICO OBTIDAS COM DIFERENTES PROTOCOLOS DE AQUISIÇÃO

Exame de Defesa apresentado ao Programa de Pós-Graduação em Clínica Odontológica, da Faculdade de Odontologia da Universidade Federal de Juiz de Fora, como requisito para obtenção do título de Mestre. Área de concentração em Clínica Odontológica.

Aprovada em:___/___/___

Banca examinadora

_____

Profa. Dra. Karina Lopes Devito
Universidade Federal de Juiz de Fora

_____

Profa. Dra. Francielle Silvestre Verner
Universidade Federal de Juiz de Fora/Campus GV

_____

Prof. Dr. Sérgio Lúcio Pereira de Castro Lopes
Universidade Estadual Paulista

“O correr da vida embrulha tudo, a vida é assim: Esquenta e esfria, aperta e daí afrouxa, sossega e depois desinquieta. O que ela quer da gente é coragem. Ser capaz de ficar alegre e mais alegre no meio da alegria, e ainda mais alegre no meio da tristeza...”

João Guimarães Rosa

DEDICATÓRIA

*Aos meus filhos **Italo** e **Enrico**, amor infinito e incondicional.*

AGRADECIMENTOS

Agradeço à **Universidade Federal de Juiz de Fora**, *na pessoa do Reitor, Prof. Dr. Marcus Vinicius David.*

À **Faculdade de Odontologia** *da Universidade Federal de Juiz de Fora, na pessoa da senhora diretora Profa. Dra. Maria das Graças de Afonso Miranda Chaves, pela oportunidade e por me oferecer condições para o meu crescimento pessoal e profissional.*

Ao **Programa de Pós-Graduação em Clínica Odontológica**, *na pessoa do Prof. Dr. Antônio Márcio Resende do Carmo, pela contribuição intelectual a mim transmitida.*

À **FAPEMIG e CAPES - Coordenação de Aperfeiçoamento de Pessoal de Nível Superior** *pelo auxílio financeiro recebido em momentos durante o Mestrado, possibilitando a realização da pesquisa.*

Aos Professores que compuseram minha banca de qualificação – Prof. Dr. **Eduardo Machado Vilela** *e Profa. Dra.* **Neuza Maria Souza Picorelli Assis**, *por terem contribuído de forma tão positiva e carinhosa com sugestões apresentadas que valeram para o aprimoramento desse trabalho.*

Aos Professores participantes da banca de defesa – Profa. Dra. **Francielle Silvestre Verner** *e Prof. Dr.* **Sérgio Lúcio Pereira de Castro Lopes**, *por gentilmente aceitarem o convite e pela disponibilidade em estarem presentes nesse dia, Obrigada!*

Ao Professor **Marcus Vinícius Queiroz de Paula** *por fazer parte dessa caminhada na Radiologia, Obrigada!*

A secretaria do Programa de Pós-Graduação em Clínica Odontológica, representada por **Cláudio** *e* **Letícia,** *pela dedicação com a qual trabalham sempre solícitos e eficientes!*

À minha orientadora, Profa. Dra. **Karina Lopes Devito***, com a devida admiração, carinho e respeito o meu muito obrigado! Obrigada por ser exemplo e incentivo no caminho da docência e da radiologia, obrigada pelas inúmeras vezes a disposição para transmitir seu conhecimento e sanar minhas dúvidas e inseguranças! Por emprestar sua sala e confiança com paciência e zelo (O Enrico também agradece!) obrigada! Pelo apoio e amizade! Por corrigir e advertir, mas acima de tudo pela oportunidade de conviver esses anos com a pessoa e profissional tão admirável. Pelos cafés, choros e risos! Que Deus abençoe sempre seu caminho! Minha sincera gratidão!*

A **Deus***, acima de todas as coisas, obrigada por ser chama e luz em meu coração, sempre segurando minha mão e me levando aos caminhos que devo seguir! Que minha vontade sempre esteja de acordo com a sua Senhor! Sem a fé e a gratidão eu não seria nada!*

Aos meus amados avós **Zico** *e* **Geny Procacci Castilho,** *exemplos de fé, virtude e caráter, pela força e ternura transmitida no educar, me fazendo crescer nas lutas com resignação e sem desistir! Por me ensinarem que o que damos, dizemos e mostramos nem sempre é alcançado pelo outro com a mesma mensagem, e por isso é necessário paciência e perdão em todas as coisas.*

Ao meu **pai***, que junto a Deus esta, obrigada! Sorria comigo! Seja luz em meu caminho!*

Aos meus **irmãos e sobrinhos** *mesmo na distancia são conforto ao coração!*

Ao **Paulo** *por ser paciente com minha jornada, por aceitar meus sonhos mesmo sem entender, por ser apoio, pai, amigo, amor. Por toda paciência e espera, porque nos melhores e nos piores momentos somos nós dois juntos o que transforma e edifica nosso lar, casamento, filhos e vida! Por fazer jus ao nosso "Dia Branco". Obrigada!*

Aos meus filhos **Ítalo e Enrico**, *agradeço por serem motivação, o incentivo mais profundo e terno! Nada no mundo se compara a força que o existir de filhos é capaz de produzir no coração de uma mãe! Vocês são amor e energia! Peço desculpa pela minha ausência e correria nessa jornada, foi pra melhor e por vocês, acreditem!*

À amiga **Alessiana**, *obrigada por fazer parte dessa jornada e de tantas outras! Em nossa amada radiologia e no caminhar do mestrado obrigada pelo apoio, guia e incentivo desde sempre! Amigos são presentes de Deus! Amigo é doação sem esperar nada em troca e receber um mundo! É ver o outro com todos os seus defeitos e enxergar além, com o coração, sabendo que ele pode ser melhor que tudo isso!*

A todos os **colegas do mestrado** *e as* **companheiras de tomógrafo Alessiana, Letícia, Isabela e Larissa,** *agradeço a oportunidade de convivência, trocas e amizade.*

Sou grata a todos nesse caminho, aos que dificultaram ou suavizaram! De certo fizeram a diferença! Muito obrigada!

FARDIM, K.A.C. **Quantificação de artefatos metálicos produzidos por implantes dentários em imagens de tomografia computadorizada de feixe cônico obtidas com diferentes protocolos de aquisição**. Juiz de Fora (MG), 2018. 61 f. Apresentação da Dissertação (Mestrado em Clínica Odontológica) - Faculdade de Odontologia, Universidade Federal de Juiz de Fora (MG).

RESUMO

O objetivo do trabalho foi quantificar, em imagens de tomografia computadorizada de feixe cônico (TCFC) obtidas com diferentes protocolos, os artefatos metálicos produzidos por implantes de titânio instalados em diferentes regiões da mandíbula. Os implantes foram instalados em quatro diferentes regiões (incisivo, canino, pré-molar e molar) de um *phamtom* e submetidos a exames de TCFC com variação da posição do objeto no interior do FOV (central, anterior, posterior, direita e esquerda), variação do FOV (6 x 13 e 12 x 13 cm) e do tamanho do voxel (0,25 e 0,30 mm). Um corte axial da região cervical de cada implante foi selecionado para quantificação. Os testes de Kruskal-Wallis e Student-Newman-Keuls foram utilizados para comparação das regiões dos dentes e entre as diferentes posições do *phantom* dentro do FOV. O teste de Wilcoxom foi utilizado para comparar a variação de tamanho do FOV e voxel. O teste ANOVA fatorial para avaliar a interação entre as variáveis do estudo. A região de incisivo apresentou a maior quantidade de artefatos, em comparação as outras regiões ($p=0,0315$). Não houve diferença significativa na variação da posição do *phantom* dentro do FOV ($p=0,7418$). O FOV menor produziu mais artefatos ($p<0,0001$). Ao comparar as imagens produzidas com diferentes resoluções, o menor voxel produziu mais artefatos ($p<0,0001$). Os artefatos metálicos sofrem influência do tamanho do FOV e do voxel, além da região anatômica. A variação da localização do *phantom* no interior do FOV não alterou a quantidade de artefatos.

PALAVRAS-CHAVES: tomografia computadorizada de feixe cônico, implante dentário, artefato metálico, posição, voxel, campo de visão.

FARDIM, K.A.C. **Quantification of metallic artifacts produced by dental implants in cbct images obtained using different acquisition protocols**Juiz de Fora (MG), 2018. 61 f. Apresentação da Dissertação (Mestrado em Clínica Odontológica) - Faculdade de Odontologia, Universidade Federal de Juiz de Fora (MG).

ABSTRACT

The objective of the present study was to quantify the metal artifacts produced by titanium implants installed in different regions of the mandible in cone beam computed tomography (CBCT) images obtained with different protocols. The implants were placed in four different regions (incisor, canine, premolar and molar) of a phamtom and subjected CBCT tests with variation of the position of the object inside the FOV (central, anterior, posterior, right and left); FOV variation (6 x 13 and 12 x 13 cm) and voxel size (0.25 and 0.30 mm). An axial section of the cervical region of each implant was selected for quantification. The Kruskal-Wallis and Student-Newman-Keuls tests were used to compare the teeth regions and between the different positions of the phantom within the FOV. The Wilcoxom test was used to compare changes in FOV and voxel size. Factorial ANOVA was used to evaluate interactions between the study variables. The incisor region had the highest number of artifacts, compared to other regions ($p = 0.0315$). No significant difference was found when varying the position of the phantom within the FOV ($p = 0.7418$). The smaller FOV produced more artifacts ($p < 0.0001$). Comparison of the images produced with different resolutions revealed that the smaller voxel produced more artifacts ($p < 0.0001$). Metallic artifacts are influenced by FOV and voxel size as the anatomical region. Variation of the phantom location within the FOV did not affect the number of artifacts generated.

KEYWORDS: *cone beam computed tomography, dental implant, metal artifact, position, voxel, field of view.*

LISTA DE ABREVIATURAS E SIGLAS

Bit	*Binary digit*
CAPES	Coordenação de Aperfeiçoamento de Pessoal de Nível Superior
TCFC	*Tomografia computadorizada de feixe cônico*
cm	Centímetros
DICOM	*Digital imaging and communications in medicine*
DPR	*Desvio padrão real*
DPT	Desvio padrão teórico máximo
et al	*Et alii*
EUA	Estados Unidos da América
FO	Faculdade de Odontologia
FOV	*Field of View*
SP	*São Paulo*
kV	Quilovolt
mA	Miliampère
mm	Milímetro
RJ	Rio de Janeiro
ROI	*Region of interest / Região de interesse*
SIN	Sistema de implante
Mean SD	*Standard Deviation / Desvio Padrão*
SPSS	*Statistical Package for Social Sciences*
TCFC	Tomografia computadorizada de feixe cônico
UFJF	Universidade Federal de Juiz de Fora
USA	*United States of America*
ICC	*Coeficiente de correlação Intraclasse*

LISTA DE SÍMBOLOS

-	Menos
%	Por cento
/	Dividido
<	Menor
=	Igual
≤	Menor igual
P	Nível de significância
r	Coeficiente de Pearson
x	Vezes / versus

LISTA DE ILUSTRAÇÕES

LISTA DE ANEXOS

SUMÁRIO

1 INTRODUÇÃO

O exame de tomografia computadorizada de feixe cônico (TCFC) é amplamente utilizado na Odontologia, especialmente na Implantodontia (SCHULZE et al., 2011., BEZERRA et al., 2015), sendo uma ferramenta útil no diagnóstico e planejamento do tratamento, permitindo detalhar a localização de estruturas anatômicas, morfologia e dimensões ósseas (DRAENERT et al., 2007; ESMAEILI et al., 2012; BECHARA et al., 2013; ESMAEILI et al., 2013; KAMBUROGLU et al., 2013; NAGARAJAPPA et al., 2015, SANCHO-PUCHADES et al., 2015).

Por ser um exame tridimensional, a TCFC é indicada no acompanhamento pós-operatório de implantes dentários para monitoração da regeneração óssea, avaliação de possíveis perdas de osso marginal e sinais de falha na osseointegração (SANCHO-PUCHADES et al., 2015). Porém, em áreas com presença de implantes instalados ocorre a formação de artefatos metálicos, podendo interferir na qualidade da imagem (SCHULZE et al., 2011; BELEDELLI e SOUZA, 2012; NAGARAJAPPA et al., 2015; SANCHO-PUCHADES et al., 2015; DE AZEVEDO VAZ et al., 2016; SMEETS et al., 2017).

Artefato de imagem é definido como qualquer distorção ou erro, visualizado nos dados reconstruídos, que não está presente no objeto sob investigação (SCHULZE et al., 2011; BELEDELLI e SOUZA, 2012; KAMBUROGLU et al., 2013; KUUSISTO et al., 2015; SANCHO-PUCHADES et al., 2015;). Em geral, quando um feixe de raios X policromático passa por um objeto, os fótons de baixa energia são mais absorvidos do que os fótons de alta energia, ocorrendo um aumento da energia média e, consequentemente, o fenômeno de endurecimento do feixe. Esse fenômeno é intensificado pela presença de materiais de alta densidade física, como os metais (BECHARA et al., 2013; JAJU et al., 2013; PANJNOUSH et al., 2016).

Os artefatos provenientes de materiais metálicos contribuem para a não homogeneidade dos valores de cinza das imagens de TCFC (PAUWELS et al., 2013; MOUDI et al., 2015), pois causam uma atenuação não linear da radiação, o que resulta em uma variação do valor médio de energia do feixe de raios X. Durante o processo de reconstrução da imagem, essa atenuação não linear pode acarretar em uma redução de sua qualidade (KRATZ et al., 2012), a ponto de prejudicar o

diagnóstico, podendo levar a interpretações falso-positivas e/ou falso-negativas (DRAENERT et al., 2007; SCHULZE et al., 2010; BECHARA et al., 2012; BELEDELLI e SOUZA, 2012; ESMAEILI et al., 2013; JAJU et al., 2013; PAUWELS et al., 2013; GAMBA et al., 2014; SANCHO-PUCHADES et al., 2015;).

Assim sendo, os implantes dentários comumente usados na prática odontológica, quando presentes na região irradiada, influenciam a aquisição das imagens tomográficas, levando a formação de artefatos, que podem interferir na visualização e na avaliação do osso adjacente aos implantes, dificultando um acompanhamento pós-operatório da osseointegração (ESMAEILI et al., 2012; KRATZ et al., 2012; ESMAEILI et al., 2013; PARSA et al., 2014; SANCHO-PUCHADES et al., 2015; VASCONCELOS et al., 2017).

Alguns estudos sugerem ainda que a formação dos artefatos pode ser influenciada pela posição do objeto no interior do FOV (*field of view*), tamanho do FOV, voxel (resolução da imagem) e pelas estruturas anatômicas adjacentes (OLIVEIRA et al., 2013; VALIZADEH et al., 2015; QUEIROZ et al., 2017; MACHADO et al., 2018), porém não existe um consenso em afirmar o quanto esses fatores contribuem para a formação de artefatos gerados na presença de implantes dentários. Sendo assim, o objetivo do presente estudo é quantificar os artefatos metálicos produzidos por implantes dentários em imagens de TCFC obtidas com diferentes protocolos, a fim de que novos parâmetros de aquisição possam ser sugeridos, tentando minimizar a formação desses artefatos.

2 PROPOSIÇÃO

O objetivo no presente estudo foi quantificar, em imagens de TCFC, os artefatos metálicos produzidos por implantes dentários, comparando:

- A quantidade de artefatos produzidos entre as diferentes regiões dos dentes (incisivo, canino, pré-molar e molar);

- A quantidade de artefatos produzidos ao variar a posição do *phantom* no interior do FOV.

- A quantidade de artefatos produzidos com variação do FOV;

- A quantidade de artefatos produzidos com variação do voxel.

3 MATERIAL E MÉTODOS

3.1 DESENHO DO ESTUDO

Trata-se de um estudo experimental analítico transversal.

3.2 MATERIAL

Foram utilizados quatro implantes dentários de titânio, no tamanho 3,75 x 13 mm, do tipo hexágono externo (SIN, São Paulo, SP, Brasil). Esses implantes foram instalados em uma mandíbula desenvolvida em poliuretano e bário (Nacional Ossos, Jaú, SP, Brasil), que permite a obtenção de uma densidade radiográfica próxima a do osso mandibular. A face vestibular do *phantom* foi coberta com 15 mm de espessura de cera utilidade (Technew, Rio de Janeiro, RJ, Brasil) para simulação de tecido mole.

3.3 MÉTODO

Do lado direito do *phantom,* escolhido aleatoriamente*,* foram removidos os dentes com auxílio da broca maxicut (Wilcos, Petrópolis, RJ, Brasil) em motor de baixa rotação. Após a remoção dos dentes, os implantes foram instalados na mandíbula isoladamente, em cada uma das regiões avaliadas (incisivo, canino, pré-molar e molar), ou seja, o *phantom* possuía apenas um implante instalado durante as aquisições.

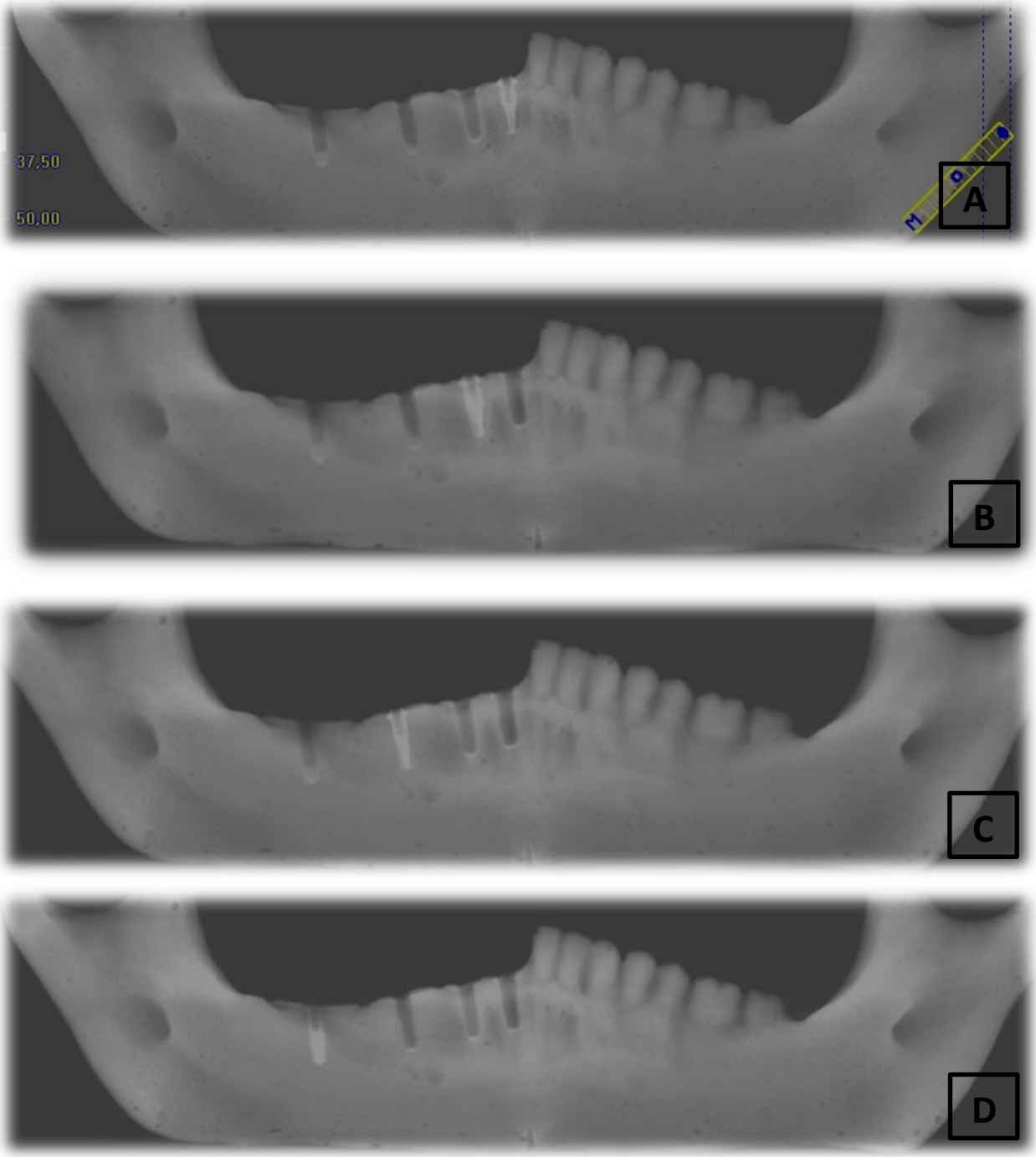

Figura 1. Cortes panorâmicos de TCFC evidenciando implantes instalados na região de dentes A. região de incisivos; B. região de canino; C. região de pré-molares; D. região de molares.

Fonte: O autor.

O *phantom* (mandíbula encerada com os implantes instalados) foi submetido a 80 aquisições de TCFC utilizando-se o tomógrafo I-Cat Next Generation (Imaging Sciences International, Hatfield, Pensilvânia, EUA), com 120 kV, 8 mA e 360° de rotação. As aquisições foram realizadas com a variação da posição do objeto no interior do FOV (central, anterior, posterior, direita e esquerda), com a variação do tamanho do FOV (6 x 13 e 12 x 13 cm) e do tamanho do voxel (0,25 e 0,30 mm). Assim sendo, cada implante (instalado em uma região específica) foi escaneado 20 vezes. O Quadro 1 ilustra as variáveis do estudo.

Quadro 1. Variáveis do estudo

Região	**Posição**	**FOV**	**Voxel**
Incisivo	Central	Pequeno (6 x 13 cm)	0,25 mm
Canino	Anterior	Grande (12 x 13 cm)	0,30 mm
Pré-molar	Posterior		
Molar	Direita		
	Esquerda		

Fonte: O autor

3.4 SELEÇÃO DOS CORTES TOMOGRÁFICOS

Após a aquisição dos exames, imagens axiais descomprimidas, em formato DICOM (*Digital Imaging and Communications in Medicine*), foram visualizadas no *software* ImageJ (U.S. *National Institutes of Health*, Bethesda, Maryland, EUA) para seleção do corte cervical de cada implante, região mais comum de perda óssea peri-implantar, onde foram quantificados os artefatos. O corte cervical padrão foi definido como aquele localizado a 3 mm da base do implante.

3.5 QUANTIFICAÇÃO DOS ARTEFATOS METÁLICOS

Para a quantificação dos artefatos metálicos também foi utilizado o *software* ImageJ (U.S. *National Institutes of Health*, Bethesda, Maryland, EUA). No corte cervical selecionado anteriormente, foi construída uma ROI (*region of interest* - região de interesse), com 10 mm de diâmetro e formato circular. Essa ROI abrangeu toda a região do implante além do tecido ósseo adjacente, onde o centro da ROI

coincidiu com o centro do implante. Para cada ROI selecionada, foram quantificados os artefatos presentes baseando-se na metodologia de Pauwels et al. (2013). Ainda no *software* ImageJ, por meio das ferramentas "*Analyze* – *Histogram*", foram determinados os valores mínimo e máximo de tons de cinza para calcular o desvio padrão real (DPR). O cálculo matemático do DPR foi realizado no programa Excel, versão 2010 (Windows XP, Microsoft, EUA).

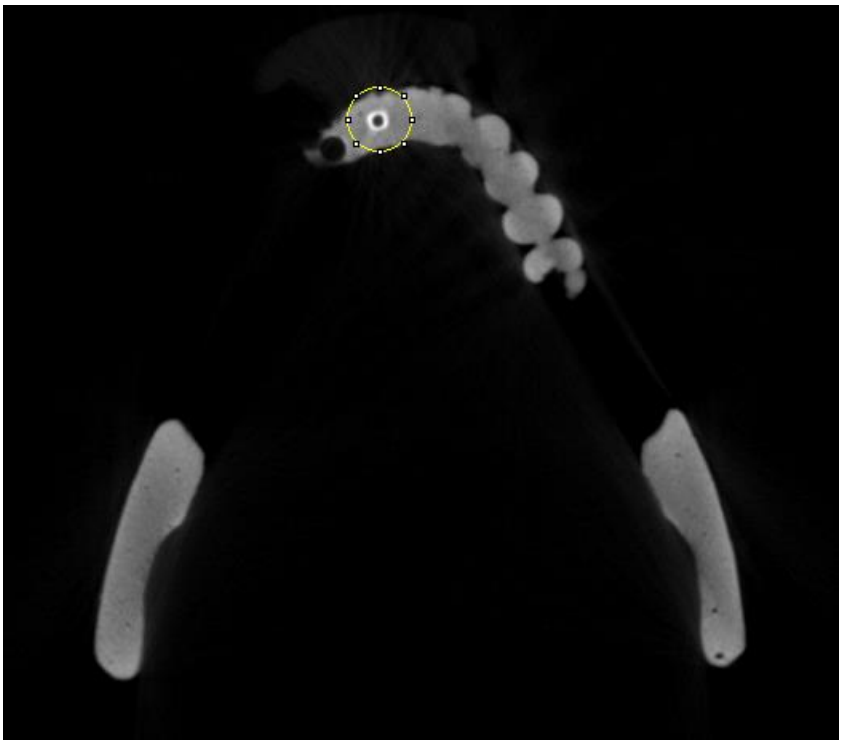

Figura 2 Corte axial cervical do implante na região de incisivo com o posicionamento da ROI definida no ImageJ.

Fonte: O autor.

Utilizando-se uma escala de 16 bits (65.536 valores de cinza), já que as imagens geradas a partir do tomógrafo utilizado nesse estudo possuem essa característica, foi determinado o desvio padrão teórico máximo (DPT), cujo valor é a metade dos valores de cinza de uma imagem de 16 bits, ou seja, 32.768. Foi considerado o valor de 32.768 tons de cinza, uma vez que metade dos voxels de uma imagem é preto e metade é branco, assim o DPT máximo deveria ser exatamente a metade dos valores de cinza de uma determinada imagem. Posteriormente o DPR foi convertido em uma porcentagem do DPT máximo, onde

valores mais elevados indicam artefatos mais pronunciados. O cálculo foi realizado da seguinte forma:

(DPR / DPT máximo) x 100 = quantificação de artefato

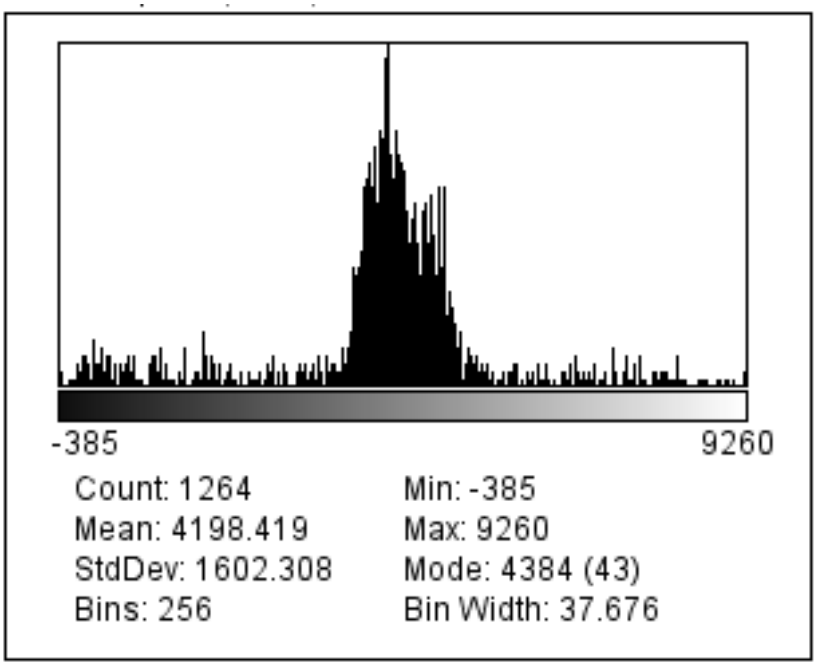

Figura 3 Histograma do software ImageJ evidenciando os valores mínimo e máximo de cinza.

Fonte: O autor.

A aquisição dos exames tomográficos, seleção dos cortes cervicais de cada implante, bem como a quantificação dos artefatos foi realizada por um único examinador, radiologista, experiente em imagens de TCFC.

Para mensurar a reprodutibilidade do método, 20% dos exames foram avaliados em dois momentos distintos, com intervalo de duas semanas entre eles, para o cálculo da concordância intraobservador.

3.6 TRATAMENTO ESTATÍSTICO

Os dados obtidos foram analisados estatisticamente no programa Statistical Package for Social Sciences (SPSS, version 15.0; IBM Corp, Armonk, New York, EUA). O nível de significância adotado foi de 5% ($p \leq 0,05$). Os testes de Kruskal-Wallis e Student-Newman-Keuls foram utilizados para comparação entre as regiões dos dentes e entre as diferentes posições do *phantom* dentro do FOV. O teste de Wilcoxom foi utilizado para comparar a variação de tamanho do FOV e voxel. O teste ANOVA fatorial foi usado para avaliar a interação ente as variáveis do estudo. A concordância intraobservador foi calculada pelo coeficiente de correlação intraclasse (ICC).

4 ARTIGO

O artigo a seguir está apresentado nas normas do periódico *Dentomaxillofacial Radiology* classificado no Qualis da CAPES (Coordenação de Aperfeiçoamento de Pessoal de Nível Superior), na Área de Avaliação de Odontologia, como A1 (ANEXO A). O comprovante de submissão do artigo ao periódico, datado de 27 de junho de 2018, está apresentado no ANEXO B.

QUANTIFICAÇÃO DE ARTEFATOS METÁLICOS PRODUZIDOS POR IMPLANTES DENTÁRIOS EM IMAGENS DE TOMOGRAFIA COMPUTADORIZADA DE FEIXE CÔNICO OBTIDAS COM DIFERENTES PROTOCOLOS DE AQUISIÇÃO

Authors:

Karolina Aparecida Castilho Fardim*

Alessiana Helena Machado*

Letícia Queiroz Mauad*

Neuza Maria Souza Picorelli Assis**

Bruno Salles Sotto-Maior***

Karina Lopes Devito**

Authors' affiliations:

* Master's Program in Dental Clinic, School of Dentistry, Federal University of Juiz de Fora, Juiz de Fora, Minas Gerais, Brazil.

** Department of Dental Clinic, School of Dentistry, Federal University of Juiz de Fora, Juiz de Fora, Minas Gerais, Brazil.

*** Department of Restorative Dentistry, School of Dentistry, Federal University of Juiz de Fora, Juiz de Fora, Minas Gerais, Brazil.

Running title:

Quantificação dos artefatos metálicos produzidos por implantes em TCFC

Corresponding author:

Karina Lopes Devito

Department of Dental Clinic, School of Dentistry, Federal University of Juiz de Fora, Campus Universitário, s/n.

CEP: 36036-900 - Juiz de Fora, MG, Brazil

E-mail: karina.devito@ufjf.edu.br

Key Words:

Cone beam computed tomography, dental implant, metal artifact; position, voxel; field of view.

QUANTIFICATION OF METALLIC ARTIFACTS PRODUCED BY DENTAL IMPLANTS IN CBCT IMAGES OBTAINED USING DIFFERENT ACQUISITION PROTOCOLS

Abstract

Objective: To evaluate cone beam computed tomography (CBCT) images obtained using different protocols to quantify metallic artifacts produced by dental implants installed in different mandibular tooth regions.

Materials and Methods: Titanium implants installed in four different regions (incisor, canine, premolar and molar) of an artificial mandible were subjected to CBCT examinations with the object in different positions within the field of view (FOV) (central, anterior, posterior, right and left) and with different FOV sizes (6 x 13 and 12 x 13 cm) and voxel sizes (0.25 to 0.30 mm). An axial section of the cervical region of each implant was selected for artifact quantification. The Kruskal-Wallis and Student-Newman-Keuls tests were used to compare the tooth regions and the different positions of the phantom within the FOV. The Wilcoxon test was used to compare changes in FOV and voxel size. Factorial ANOVA was used to evaluate interactions between the study variables.

Results: The incisor region had the highest number of artifacts compared to the other regions ($p=0.0315$). No significant difference was found when varying the position of the phantom within the FOV ($p=0.7418$). The smaller FOV produced more artifacts ($p<0.0001$). Comparison of the images produced with different resolutions revealed that the smaller voxel produced more artifacts ($p<0.0001$).

Conclusions: Metallic artifacts are affected by FOV and voxel size as well as the anatomical region. Variation of the phantom location within the FOV did not affect the number of artifacts generated.

Keywords: Cone-beam computed tomography; dental implants; artifacts; position; voxel; field of view.

Introduction

Cone beam computed tomography (CBCT) examinations are widely used in dentistry, especially in implantology, and serve as a useful tool in diagnosis and treatment planning. They allow identification of anatomical structures, morphology, and bone dimensions.[1-5]

As a method of three-dimensional examination, CBCT is indicated in the postoperative follow-up of dental implants for bone regeneration monitoring, evaluation of possible marginal bone loss and identification of signs of osseointegration failure.[5] However, in regions with installed implants, metallic artifacts can form, which may affect image quality.[4-7]

An image artifact is defined as any distortion or error observed in the reconstructed data that is not present in the object under investigation.[3, 5, 8] In general, when a polychromatic X-ray beam passes through an object, more low-energy photons are absorbed than high-energy photons, resulting in increased mean energy and consequently the beam hardening phenomenon. This phenomenon is intensified by the presence of high-physical-density materials such as metals.[1, 9, 10]

Artifacts from metallic materials contribute to the inhomogeneity of gray values in CBCT images[11, 12] because they cause nonlinear attenuation of the radiation, resulting in variation in the mean value of the X-ray energy beam. During image reconstruction, this nonlinear attenuation can result in a reduction in quality[13], which may compromise diagnosis and lead to false-positive and/or false-negative interpretations.[2, 5, 9, 11, 14, 15]

Dental implants commonly used in dental practice, when present in the irradiated region, can affect tomographic image acquisition and lead to the formation

of artifacts, which may interfere with viewing and evaluation of bone adjacent to the implant, hindering postoperative osseointegration monitoring.[2, 5, 13, 16, 17]

Some studies even suggest that artifact formation can be affected by the object's position within the field of view (FOV), FOV size, voxel size (image resolution) and adjacent anatomical structures.[18-21] However, no consensus is available regarding the extent to which these factors contribute to the formation of artifacts generated in the presence of dental implants. Therefore, the objective of this study is to quantify the metallic artifacts produced by dental implants in CBCT images obtained using different protocols (variations in FOV, voxel size and positioning of the object within the FOV) to determine new acquisition parameter suggestions and thus minimize the formation of these artifacts.

Materials and methods

This was a cross-sectional analytical experimental study conducted at the School of Dentistry, Federal University of Juiz de Fora (Universidade Federal de Juiz de Fora – UFJF), located in Juiz de Fora, Minas Gerais, Brazil.

Four 3.75- x 13-mm external hexagon titanium implants were used (SIN, São Paulo, SP, Brazil). These implants were installed in a polyurethane and barium model mandible (Nacional Ossos, Jau, SP, Brazil), which provides a radiographic density similar to that of the mandibular bone. The buccal surface of the phantom was covered with 15-mm-thick utility wax (Technew, Rio de Janeiro, RJ, Brazil) for soft tissue simulation.

Initially, the teeth from the phantom's right side were removed with the aid of a MaxiCut drill (Wilcos, Petrópolis, RJ, Brazil) at low rotation speed. After removal of the teeth, the implants were installed in the mandible alone in each of the evaluated

regions (incisor, canine, premolar and molar); that is, the phantom had only one implant installed during the acquisitions.

The phantom was subjected to 80 CBCT acquisitions using an I-Cat Next Generation scanner (Imaging Sciences International, Hatfield, Pennsylvania, USA) at 120 kV, 8 mA and 360° rotation. The acquisitions were performed while varying the object's position within the FOV (central, anterior, posterior, right and left), with variations in FOV size (6 x 13 and 12 x 13 cm) and voxel size (0.25 and 0.30 mm). Each implant (installed in a specific region) was therefore scanned 20 times.

After acquisition of the images, uncompressed axial images in DICOM (Digital Imaging and Communications in Medicine) format were viewed using ImageJ software (U.S. National Institutes of Health, Bethesda, Maryland, USA) to select the cervical section of each implant, the most common region of peri-implant bone loss, where the artifacts were quantified. A standard cervical section was defined as the section located 3 mm from the base of the implant.

ImageJ software was also used to quantify the metallic artifacts. A region of interest (ROI) with a 10-mm diameter and a circular shape was constructed in the previously selected cervical section. This ROI covered the entire implant region as well as the adjacent bone tissue, where the ROI's center coincided with the center of the implant. The artifacts present in each selected ROI were counted based on the method described by Pauwels et al[11]. ImageJ software was also used to determine the minimum and maximum grayscale values required to calculate the actual standard deviation (ASD) using the "*Analyze-Histogram*" tool. The ASD was calculated in Excel, version 2010 (Windows XP, Microsoft, USA).

Using a 16-bit scale (65,536 gray values) because the images generated by the CT scanner used in this study had this characteristic, the maximum theoretical

standard deviation (TSD) was calculated, the value of which is half of the gray values of a 16-bit image, or 32,768. The value of 32,768 shades of gray was adopted, as half of the voxels of an image are black and half are white; therefore, the maximum TSD should be exactly half of the gray values of a particular image. Subsequently, the ASD was converted into a percentage of the maximum TSD, where higher values indicate more pronounced artifacts. The calculation was performed as follows:

(ASD/maximum TSD) x 100 = quantification of artifacts

Tomographic examination, selection of cervical sections for each implant and artifact quantification were performed by a single examiner, who was a radiologist with experience in interpreting CBCT images.

To measure the reproducibility of the method, 20% of the exams were evaluated at two different times with a two-week interval between them to calculate intraobserver agreement.

The obtained data were statistically analyzed using the Statistical Package for Social Sciences (SPSS, version 15.0; IBM Corp, Armonk, New York, USA). The significance level adopted was 5% ($p \leq 0.05$). The Kruskal-Wallis and Student-Newman-Keuls tests were used to compare the tooth regions and the different positions of the phantom within the FOV. The Wilcoxon test was used to compare changes in FOV and voxel size. Factorial ANOVA was used to evaluate interactions between the study variables. Intraobserver agreement was calculated using the intraclass correlation coefficient (ICC).

Results

Excellent intraobserver reproducibility was observed for artifact quantification (ICC 0.9927; $p<0.0001$). Tables 1 and 2 show the values of the artifacts found for the CBCT images of dental implants installed in different regions. The images were obtained by varying the positions of the phantom inside the FOV and the FOV and voxel size. Figure 1 shows various axial slices of the implants and their respective artifacts.

Table 1

Table 2

Figure 1

The results show that when the number of artifacts was compared among the four tooth regions (incisor, canine, premolar and molar), the incisor region had the largest number of artifacts (Table 3).

Table 3

When comparing the number of artifacts produced among the different phantom positions inside the FOV, no significant differences were found (Table 4).

Table 4

Comparison of the number of artifacts produced by implants in CBCT images with different FOV sizes revealed that the smaller FOV produced more artifacts (Table 5).

Table 5

Comparison between images produced with different resolutions revealed that the smaller voxel produced more artifacts (Table 6).

Table 6

Regardless of the evaluated region (incisors, canines, premolars or molars), the factorial ANOVA results showed no significant interactions between the position of the phantom within the FOV, FOV size and voxel size ($p>0.05$).

Discussion

Cone beam computed tomography (CBCT) has become an indispensable diagnostic modality in dental practice, especially in the planning of dental implants.[14, 22] However, the presence of high-physical-density objects, such as titanium dental implants, within the field of view leads to the formation of metallic artifacts. During image acquisition, dental implants and other metallic objects within the FOV absorb a greater number of low-energy X-ray photons due to their high atomic number. This increases the mean energy of the X-ray beam and thereby produces an effect known as "beam hardening".[5, 11, 14, 18, 19]

These metallic artifacts can affect image quality and are detrimental to the diagnosis of pathological conditions, such as fenestrations or peri-implant dehiscence[6, 17], reducing image accuracy.[14, 16, 18, 21]

This study quantified the metallic artifacts produced in CBCT images by titanium dental implants and considered certain factors that contribute to variations in gray values, such as different anatomical regions, the object's position within the FOV, FOV size and voxel size.[18-20]

The gray values were not uniform across the entire dental arch. When the number of metallic artifacts produced was compared among the various anatomical regions (incisor, canine, premolar and molar), a greater number of artifacts was observed in the incisor region, which is consistent with previous studies.[18, 21] Most likely, variations in gray values between the different regions are due to differences in mandibular bone density and thickness. [18, 21] CBCT gray values are related to the attenuation of X-rays, which, when crossing thinner regions such as incisors, are not absorbed uniformly, causing higher grayscale variability.[18]

Parameters related to the acquisition protocol of tomographic images, such as FOV size, also affected image quality. A greater number of metallic artifacts was found in the acquisitions performed with a small FOV, probably due to the number of anatomical structures located within and outside the FOV, which affect the gray values of CT images.[5, 18, 21] In images with a small FOV, a greater presence of exo-mass exists, or anatomical structures located externally to the FOV, which are not reconstructed during the examination and lead to increased artifact formation.[14] Katsumata et al[23] also observed greater grayscale variability in images with a smaller FOV and found that this variation decreased in acquisitions with larger FOVs. However, larger FOV sizes are known to involve higher radiation doses administered to the patient. Therefore, exposing a patient to higher doses is not justifiable if no significant improvement in image quality can be achieved.[24, 25] Pauwels et al[11] observed that in general, protocols with higher radiation doses do not significantly reduce the number of artifacts. In clinical practice, if a larger FOV size is selected only to reduce the number of artifacts, then the voxel size should be increased to compensate for the radiation dose; however, image quality is reduced as a result, with lower spatial resolution.[20]

When comparing images produced at two different resolutions, the smaller voxel size was found to produce a greater number of artifacts, which differs from Pauwels et al's[11] results in which varying the voxel size did not affect gray values. One possible explanation for the variation in the number of artifacts found for different voxel sizes may be related to image noise. Voxels of different sizes detect X-ray photons differently. A smaller voxel will not detect as many photons as a larger voxel due to a reduced signal and increased noise. In turn, larger voxels can detect more energy and thus improve the signal.[17]

According to the literature, metallic artifacts are also affected by the location of the object within the FOV.[19, 24, 26] In this study, when quantifying artifacts, no significant differences were observed when the phantom's position within the FOV was changed from a central position to anterior, posterior, right and left positions. Valizadeh et al[19] assessed the diagnosis of vertical root fractures in teeth with intracanal metallic pins and concluded that the central position produced the highest sensitivity values (better diagnosis of fractures) and that the "3 o'clock" position (right position) produced the highest specificity values (better diagnosis of healthy teeth).

An alternative for minimizing metallic artifacts is the use of metallic artifact reduction (MAR) algorithms. Several studies have used these artifact reduction tools to improve the diagnosis of peri-implant bone defects or root fractures.[6, 27] Although Bechara et al[15] reported improved image quality after application of these algorithms, no consensus is available regarding the reliability of this tool.[1, 3, 6, 11, 16, 27]

Given the aforementioned results, the metallic artifacts produced by dental implants are affected by varying the FOV, voxel size and anatomical region. More research on artifact quantification with other equipment is needed to assist in the development of future generations of CT scanners, better MAR algorithms and image processing software in a constant effort to provide better image quality and lower radiation doses.

.

References

1. Bechara B, Alex McMahan, C, Moore, WS, Noujeim M, Teixeira FB, Geha H. Cone beam CT scans with and without artefact reduction in root fracture detection of endodontically treated teeth. *Dentomaxillofac Radiol* 2013; **42**: 20120245.
2. Esmaeili F, Johari M, Haddadi P. Beam hardening artifacts by dental implants: comparison of cone-beam and 64-slice computed tomography scanners. *Dent Res J* 2013; **10**: 376-81.
3. Kamburoglu K, Kolsuz E, Murat S, Eren H, Yüksel S, Paksoy CS. Assessment of buccal marginal alveolar peri-implant and periodontal defects using a cone beam CT system with and without the application of metal artefact reduction mode. *Dentomaxillofac Radiol* 2013; **42**: 20130176.
4. Nagarajappa AK, Dwivedi N, Tiwari R. Artifacts: the downturn of cbct image. *J Int Soc Prev Community Dent* 2015; **5**: 440-5.
5. Sancho-Puchades M, Hämmerle CH, Benic GI. In vitro assessment of artifacts induced by titanium, titanium-zirconium and zirconium dioxide implants in cone beam computed tomography. *Clin Oral Implants Res* 2015; **26**: 1222-8.
6. de-Azevedo-Vaz SL, Peyneau PD, Ramirez-Sotelo LR, Vasconcelos KF, Campos PS, Haiter-Neto F. Efficacy of a cone beam computed tomography metal artifact reduction algorithm for detection of peri-implant fenestrations and dehiscences. *Oral Surg Oral Med Oral Pathol Oral Radiol* 2016; **121**: 550-
7. Smeets R, Schöllchen M, Gauer T, Aarabi G, Assaf AT, Rendenbach C, et al. Artefacts in multimodal imaging of titanium, zirconium and binary titanium-zirconium alloy dental implants: an in vitro study. *Dentomaxillofac Radiol* 2017; **46**: 20160267.

8. Kuusisto N, Vallittu PK, Lassila LV, Huumonen S. Evaluation of intensity of artefacts in CBCT by radio-opacity of composite simulation models of implants in vitro. *Dentomaxillofac Radiol* 2015; **44**: 20140157.
9. Jaju PP, Jain M, Singh A, Gupta A. Artefacts in cone beam CT. *Open J Stomatol* 2013; **3**: 292-7.
10. Panjnoush M, Kheirandish Y, Kashani PM, Jakhar HB, Younesi F, Mallahi M. Effect of expousure parameters on metal artifacts in cone beam computed tomography. *J Dent* 2016; **13**: 143-50.
11. Pauwels R, Stamatakis H, Bosmans H, Bogaerts R, Jacobs R, Hormer K, et al. Quantification of metal artifacts on cone beam computed tomography images. *Clin Oral Implants Res* 2013; **24**: 94-9.
12. Moudi E, Haghanifar S, Madani Z, Bijani A, Nabavi ZS. The effect of metal on the identification of vertical root fractures using different fields of view in cone beam computed tomography. *Imaging Sci Dent* 2015; **45**: 147-51.
13. Kratz B, Weyers I, Buzug TM. A fully 3D approach for metal artifact reduction in computed tomography. *Med Phys* 2012; **39**: 7042-54.
14. Schulze RK, Berndt D, d'Hoedt B. On cone-beam computed tomography artifacts induced by titanium implants. *Clin Oral Implants Res* 2010; **21**:100-7.
15. Bechara BB, Moore WS, McMahan CA, Noujeim M. Metal artefact reduction with cone beam TC: an in vitro study. *Dentomaxillofac Radiol* 2012; **41**: 248-5.
16. Parsa A, Ibrahim N, Hassan B, Syriopoulos K, van der Stelt P. Assessment of metal artefact reduction around dental titanium implants in cone beam CT. *Dentomaxillofac Radiol* 2014; **43**: 20140019.
17. Vasconcelos TV, Bechara BB, McMahan CA, Freitas DQ, Noujeim M. Evaluation of artifacts generated by zirconium implants in cone-beam

computed tomography images. *Oral Surg Oral Med Oral Pathol Oral Radiol* 2017; **123**: 265-72.

18. Oliveira ML, Tosoni GM, Lindsey DH, Mendoza K, Tetradis S, Mallya SM. Influence of anatomical location on CT numbers in cone beam computed tomography. *Oral Surg Oral Med Oral Pathol Oral Radiol* 2013; **115**: 558-64.
19. Valizadeh S, Vasegh Z, Rezapanah S, Safi Y, Khaeazifard MJ. Effect of object position in cone beam computed tomography field of view for detection of root fractures in teeth with intra-canal posts. *Iran J Radiol* 2015; **12**: e25272.
20. Queiroz PM, Santaella GM, da Paz TD, Freitas DQ. Evaluation of a metal artifact reduction tool on different positions of a metal object in the FOV. *Dentomaxillofac Radiol* 2017; **46**: 20160366.
21. Machado AH, Fardim KAC, de Souza CF, Sotto-Maior BS, Assis NMSP, Devito KL. Effect of anatomical region on the formation of metal artifacts produced by dental implants in cone beam computed tomographic images. *Dentomaxillofac Radiol* 2018; **47**: 20170281.
22. Benic GI, Sancho-Puchades M, Jung RE, Deyhle H, Hämmerle CH. In vitro assessment of artifacts induced by titanium dental implants in cone beam computed tomography. *Clin Oral Implants Res* 2013; **24**: 378-83.
23. Katsumata A, Hirukawa A, Okumura S, Naitoh M, Fujishita M, Arji E, Langlais RP. Relationship between density variability and imaging volume size in cone-beam computadorized tomographic scanning of the maxillofacial region: an in vitro study. *Oral Surg Oral Med Oral Pathol Oral Radiol Endod* 2009; **107**: 420-
24. Pauwels R, Jacobs R, Bogaerts R, Bosmans H, Panmekiate S. Reduction of scatter-induced image noise in cone beam computed tomography: effect of field of view size and position. *Oral Radiol* 2016; **121**: 188-95.

25. SEDENTEXCT Project. Radiation Protection n°. 172: Cone Beam CT for Dental and Maxillofacial Radiology. Evidence-based Guidelines. Luxembourg: European Commission Directorate-General for Energy; 2012.
26. Taylor C. Evaluation of the effects of positioning and configuration on contrast-to-noise ratio in the quality control of a 3D Accuitomo 170 dental CBCT system. *Dentomaxillofac Radiol* 2016, **45**: 20150430.
27. de Rezende Barbosa GL, Souza Melo SL, Alencar PN, Nascimento MC, Almeida SM. Performance of an artefact reduction algorithm in the diagnosis of in vitro vertical root fracture in four different root filling conditions on CBCT images. *Int Endod J* 2016; **49**: 500-8.

.

Figure Legends

Fig. 1. Examples of metal artifacts in CBCT images of dental implants in axial slices.

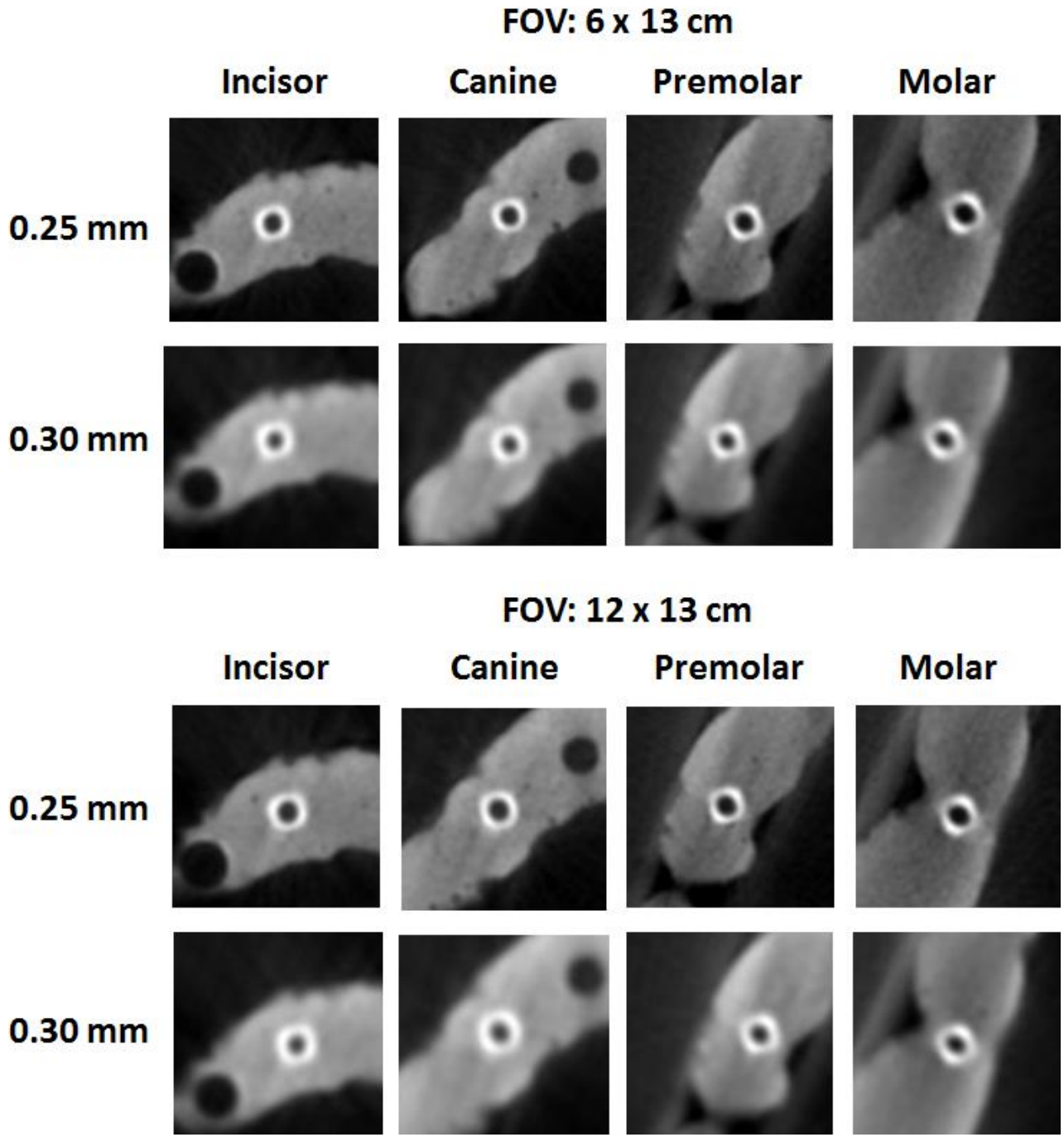
FOV: 6 x 13 cm
Incisor
Canine
Premolar
Molar
0.25 mm
0.30 mm
FOV: 12 x 13 cm
Incisor
Canine
Premolar
Molar
0.25 mm
0.30 mm

Table 1. The number of artifacts (%) produced in CBCT images obtained with a small FOV (6 x 13 cm).

		Position				
Voxel	**Region**	Central	Anterior	Posterior	Right	Left
0.25 mm	Incisor	21.08	21.61	22.89	20.68	21.77
	Canine	19.73	19.38	19.63	18.23	19.48
	Premolar	19.90	19.03	20.12	19.78	20.12
	Molar	19.70	19.12	19.37	19.17	19.53
0.30 mm	Incisor	16.62	17.01	17.40	16.40	16.24
	Canine	15.49	15.59	15.51	15.09	15.99
	Premolar	15.54	15.46	15.59	14.51	15.59
	Molar	15.97	15.99	15.62	15.61	15.36

Table 2. The number of artifacts (%) produced in CBCT images obtained with a large FOV (12 x 13 cm).

		Position				
Voxel	**Region**	Central	Anterior	Posterior	Right	Left
0.25 mm	Incisor	20.81	20.85	20.88	19.66	19.54
	Canine	18.21	17.81	18.98	17.33	18.04
	Premolar	19.43	18.58	20.59	18.79	19.08
	Molar	18.32	18.51	18.54	17.92	19.88
0.30 mm	Incisor	20.61	15.45	15.70	15.73	14.26
	Canine	14.56	14.35	15.78	13.84	14.12
	Premolar	14.72	14.80	15.78	14.41	15.12
	Molar	15.27	14.93	13.59	14.46	16.29

Table 3. Comparison of the number of artifacts produced by metallic implants installed in different regions of the mandibular teeth.

Region	Mean (SD)	Median	P value
Incisor	18.76 (2.64)	19.60 A	0.0315*
Canine	16.86 (2.03)	16.66 B	
Premolar	17.35 (2.32)	17.18 B	
Molar	17.16 (2.02)	17.10 B	

SD: standard deviation

*Medians followed by different letters indicate a significant difference according to the Kruskal-Wallis and Student-Newman-Keuls tests.

Table 4. Comparison of the number of metallic artifacts produced with different phantom positions within the FOV.

Position	Mean (SD)	Median	P Value
Central	17.87 (2.36)	18.26	
Anterior	17.40 (2.26)	17.41	
Posterior	17.87 (2.60)	17.97	0.7418*
Right	16.98 (2.24)	16.86	
Left	17.53 (2.40)	17.17	

SD: standard deviation

* No significant difference according to the Kruskal-Wallis test.

Table 5. Comparison of the number of metallic artifacts produced by implants in images obtained with different FOVs.

FOV	Mean (SD)	Median	P Value
6 x 13 cm	17.92 (2.30)	17.81	<0.0001*
12 x 13 cm	17.14 (2.34)	17.57	

SD: standard deviation

* Significant difference according to the Wilcoxon test.

Table 6. Comparison of the number of metallic artifacts produced by implants in images obtained with different voxel sizes.

Voxel	Mean (SD)	Median	P value
0.25 mm	19.55 (1.17)	19.50	<0.0001*
0.30 mm	15.51 (1.16)	15.52	

SD: standard deviation

* Significant difference according to the Wilcoxon test.

5 CONSIDERAÇÕES FINAIS

Devido ao grande prejuízo que a presença de artefatos metálicos causa em imagens de TCFC, esse estudo, que quantificou os artefatos metálicos causados por implantes dentários de titânio, indicou que a maior quantidade de artefatos está relacionada à região anterior da mandíbula, menores tamanhos de FOV e voxel. É importante ressaltar, como limitação, que o estudo foi realizado em um *phantom* ficando claro, por tanto, que condições in vitro, não fornecem uma estimativa da precisão do diagnóstico real.

REFERÊNCIAS

BECHARA, B.; MCMAHAN, C.A.; GEHA, H.; NOUJEIM, M. Evaluation of a cone beam CT artefact reduction algorithm. **Dentomaxillofac Radiol**, v. 41, n. 5, p. 422-428, 2012.

BECHARA, B.; ALEX McMAHAN, C.; MOORE, W. S.; NOUJEIM, M.; TEIXEIRA, F. B.; GEHA, H. Cone beam CT scans with and without artefact reduction in root fracture detection of endodontically treated teeth. **Dentomaxillofac. Radiol.**, v. 42, n. 5, p. 20120245, May 2013.

BELEDELLI, R., SOUZA, P.H.C. O que são e como se formam os artefatos nas imagens da tomografia computadorizada de feixe cônico. **Rev ABRO**, v. 13, n. 1, p. 2-15, 2012.

BENIC, G. I.; SANCHO-PUCHADES, M.; JUNG, R. E.; DEYHLE, H.; HÄMMERLE, C. H. *In vitro* assessment of artifacts induced by titanium dental implants in cone beam computed tomography. **Clin. Oral Implants Res.**, v. 24, n. 4, p. 378-383, Apr. 2013.

BEZERRA, I.S.; NEVES, F.S.; VASCONCELOS, T.V.; AMBROSANO, G.M.; FREITAS, D.Q. Influence of the artefact reduction algorithm of Picasso Trio CBCT system on the diagnosis of vertical root fractures in teeth with metal posts. Dentomaxillofac Radiol, v. 44, n. 6, p. 20140428, 2015.

DE AZEVEDO-VAZ, S. L; PEYNEAU, P. S; RAMIREZ-TOLEDO, L. R; VASCONCELOS, K. F; CAMPOS, P. S.; HAITER-NETO, F. Efficacy of a cone beam computed tomography metal artifact reduction algorithm for detection of peri-implant fenestrations and dehiscences. **Oral Surg. Oral Med. Oral Pathol. Oral Radiol.**, v. 121, n. 5, p. 550-556, May 2016.

DE REZENDE B, MELO SLM, ALENCAR PNB, NASCIMENTO MCC, ALMEIDA SM. Performance of na artefact reduction algorithm in the diagnosis of in vitro vertical root fracture in four diferente root filling conditions on CBCT images, **International Endodontic Journal** 2015; 49, 500–508, 2016.

DRAENERT, F. G; COPPENRATH, E.; HERZOG, P.; MÜLLER, S., MUELLER-LISSE, U. G. Beam hardening artefacts occur in dental implants with NewTom cone beam CT but not with the dental 4-row multidetector CT. **Dentomaxillofac. Radiol.**, v. 36, n. 4, p.198-203, May 2007.

ESMAEILI, F.; JOHARI, M.; HADDADI, P. Beam hardening artifacts by dental implants: comparison of cone-beam and 64-slice computed tomography scanners. **Dent. Res. J.**, v. 10, n. 3, p. 376-381, May 2013.

ESMAEILI, F.; JOHARI, M.; HADDADI, P.; VATANKHAH, M. Beam hardening artifacts: comparison between two cone beam computed tomography scanners. **J. Dent. Res. Dent. Clin. Dental Prospects**, v. 6, n. 2, p. 49-53, Spring 2012.

JAJU, P. P; JAIN, M.; SINGH, A.; GUPTA, A. Artefacts in cone beam CT. **Open J. Stomatol.**, v. 3, p. 292-297, Aug. 2013.

KAMBUROGLU, K.; KOLSUZ, E.; MURAT, S.; EREN, H.; YÜKSEL, S.; PAKSOY, C. S. Assessment of buccal marginal alveolar peri-implant and periodontal defects using a cone beam CT system with and without the application of metal artefact reduction mode. **Dentomaxillofac. Radiol.**, v. 42, n. 8, p. 20130176, Aug. 2013.

KATSUMATA A, HIRUKAWA A, OKUMURA S, NAITOH M, FUJISHITA M,NARJI E, LANGLAIS RP. Relationship between density variability and imaging volume size in cone-beam computadorized tomographic scanning of the maxillofacial region: an in vitro study, **Oral Surg Oral Med Oral Pathol Oral Radiol Endod** 2009; 107:420-425..

KRATZ, B.; WEYERS, I.; BUZUG, T. M. A fully 3D approach for metal artifact reduction in computed tomography. **Med. Phys.**, v. 39, n. 11, p. 7042-7054, Nov. 2012.

KUUSISTO, N.; VALLITTU, P. K.; LASSILA, L. V.; HUUMONEN, S. Evaluation of intensity of artefacts in CBCT by radio-opacity of composite simulation models of implants *in vitro*. **Dentomaxillofac. Radiol.**, v. 44, n. 2, p. 20140157, Feb. 2015.

MACHADO AH, FARDIM KAC, DE SOUZA CF, SOTTO-MAIOR BS, ASSIS NMSP, DEVITO KL. Effect of anatomical region on the formation of metal artifacts produced by dental implants in cone beam computed tomographic images**, Dentomaxillofacial Radiology** 2018; 47: (3):20170281.

MOUDI, E.; HAGHANIFAR, S.; MADANI, Z.; BIJANI, A.; NABAVI, Z. S. The effect of metal on the identification of vertical root fractures using different fields of view in cone beam computed tomography. **Imaging Sci. Dent.**, v. 45, n. 3, p. 147-151, Sep. 2015.

NAGARAJAPPA, A. K.; DWIVEDI, N.; TIWARI, R. Artifacts: the downturn of CBCT image. **J. Int. Soc. Community Dent.**, v. 5, n. 6, p. 440-445, Nov.-Dec. 2015.

OLIVEIRA, M. L.; TOSONI, G. M.; LINDSEY, D. H.; MENDOZA, K.;TETRADIS, S.; MALLYA, S. M. Influence of anatomical location on CT numbers in cone beam computed tomography. **Oral Surg. Oral Med. Oral Pathol. Oral Radiol.**, v. 115, n. 4, p. 558-564, Apr. 2013.

PANJNOUSH, M.; KHEIRANDISH, Y.; KASHANI, P. M.; JAKHAR H. B.; YOUNESI, F.; MALLAHI, M. Effect of Expousure parameters on metal artifacts in cone beam computed tomography. **J Dent (Tehran)**.,v.13, n.3, p. 143-150, June 2016.

PARSA, A.; IBRAHIM, N.; HASSAN, B.; SYRIOPOULOS, K.; VAN DER STELT, P. Assessment of metal artefact reduction around dental titanium implants in cone beam CT. **Dentomaxillofac. Radiol.**, v. 43, n. 7, p. 20140019, Oct. 2014.

PAUWELS, R.; STAMATAKIS, H.; BOSMANS, H.; BOGAERTS, R.; JACOBS, R.; HORNER, K.; TSIKLAKIS, K; SEDENTEXCT Project Consortium. Quantification of metal artifacts on cone beam computed tomography images. **Clin. Oral Implants Res.**, v. 24, n. A100, p. 94-99, Aug. 2013.

PAUWELS, R.; JACOBS, R.; BOGAERTS, R.; BOSMANS, H.; PANMEKIATE, S. Reduction of scatter-induced image noise in cone beam computed tomography: effect of field of view size and position. **OralRadiol.**, v. 121, n. 2, p. 188-195, Feb. 2016.

QUEIROZ, P. M; SANTAELLA, G. M.; DA PAZ, T. D.; FREITAS, D. Q. Evaluation of a metal artefact reduction tool on different positions of a metal object in the FOV. **Dentomaxillofac. Radiol.**, v. 46, n. 3, p. 20160366, Mar. 2017.

SANCHO-PUCHADES, M., HÄMMERLE, C. H., BENIC, G. I. In vitro assessment of artifacts induced by titanium, titanium-zirconium and zirconium dioxide implants in cone beam computed tomography. **Clin. Oral Implants Res.**, v. 26, n. 10, p. 1222-1228, Oct. 2015.

SEDENTEXCT Guideline Development Panel. Radiation Protection No. 172: Cone Beam CT for Dental and Maxillofacial Radiology. Evidence-based Guidelines. Luxembourg: European Commission Directorate-General for Energy; 2012.

SCHULZE, R. K.; BERNDT, D.; D'HOEDT, B. On cone-beam computed tomography artifacts induced by titanium implants. **Clin. Oral Implants Res.**, v. 21, n. 1, p.100-107, Jan. 2010.

SCHULZE, R.; HEIL, U.; GROSS, D.; BRUELLMANN, D.D.; DRANISCHNIKOW, E.; SCHWANECKE, U.; SCHOEMER, E. Artefacts in CBCT: a review. **Dentomaxillofac Radiol**, v. 40, n. 5, p. 265-273, 2011.

SMEETS, R., SCHÖLLCHEN, M., GAUER, T AARABI, G., ASSAF, A. T, RENDENBACH, C., BECK-BROISCHSITTER, B., SEMMUSCH, J., SEDLACIK, J., HEILAND, M., FIEHLER, J., SIEMONSEN, S. Artefacts in multimodal imaging of titatium, zirconium and binary titaniu-zirconium alloy dental implants: an *in vitro* study. **Dentomaxillofac. Radiol.**, v. 46, n. 2, p. 265-273, Feb. 2017.

TAYLOR C. Evaluation of the effects of positioning and configuration on contrast-to-noise ratio in the quality control of a 3D Accuitomo 170 dental CBCT system, **Dentomaxillofacial Radiology** 2016, 45, 20150430.

VALIZADEH, S.; VASEGH, Z.; REZAPANAH, S.; SAFI, Y.; KHAEAZIFARD, M. J. Effect of object position in cone beam computed tomography field of view for detection of root fractures in teeth with intra-canal posts. **Iran J. Radiol.**, v. 12, n. 4, p. 25272, Oct. 2015.

VASCONCELOS, T. V.; BECHARA, B. B.; MCMAHAN, C. A.; FREITAS, D. B.; NOUJEIM, M. Evaluation of artifacts generated by zirconium implants in cone-beam computed tomography images. **Oral Surg. Oral Med. Oral Pathol. Oral Radiol.**, v. 123, n. 2, p. 265-272, Feb. 2017.

ANEXO A – Normas para publicação

Preparing your submission

For guidelines regarding word count, figure/table count and references for all DMFR article types see here.

Authors' names and affiliations should not appear anywhere on the manuscript pages or the images (to ensure blind peer-review).

Teeth should be designated in the text using the full English terminology. In tables and figures individual teeth can be identified using the FDI two-digit system, i.e. tooth 13 is the first permanent canine in the right maxilla region.

- Author contribution statement
- Title page
- Abstract
- Main text
- References
- Tables
- Figures
- Appendices
- Supplementary material
- Units, symbols and statistics

Submit now!

Author contribution statement

DMFR requires that an author contribution statement accompany each submission, outlining the contributions of each author towards the work. A template statement can be downloaded here.

DMFR requires that for all submitted papers:

- All the authors have made substantive contributions to the article and assume full responsibility for its content; and
- All those who have made substantive contributions to the article have been named as authors.

The International Committee of Medical Journal Editors recommends the following definition for an author of a work, which we ask our authors to adhere to:

Authorship be based on the following 4 criteria [1]:

- Substantial contributions to the conception or design of the work; or the acquisition, analysis, or interpretation of data for the work; AND
- Drafting the work or revising it critically for important intellectual content; AND
- Final approval of the version to be published; AND
- Agreement to be accountable for all aspects of the work in ensuring that questions related to the accuracy or integrity of any part of the work are appropriately investigated and resolved.

1 The International Committee of Medical Journal Editors, Roles and Responsibilities of Authors, Contributors, Reviewers, Editors, Publishers, and Owners: Defining the Role of Authors and Contributors, http://www.icmje.org/roles_a.html

Title page

The title page is a separate submission item to the main manuscript and should provide the following information:

- Title of the paper. Abbreviations other than CT or MRI should not be used in the title.
- A shortened version of the title (no more than 70 characters in length, including spaces) should be provided for use as the running head. Abbreviations are permissible.
- Type of Manuscript (see all types of manuscript)
- Author names should appear **in full** (in the format: "first name, initial(s), last name), qualifications and affiliations.
- Statement indicating any source of funding or financial interest where relevant should be included.
- A cover letter or statement can be included into the title page, but please note this is not a compulsory item.

Blind title page

A blind title page should be included with the full manuscript, giving only the title (i.e. without the authors' names and affiliations), for use in the peer-review process.

Abstract

The abstract should be an accurate and succinct summary of the paper, not exceeding **250 words**. For papers containing research: the abstract should be constructed under the following subheadings:

- Objectives;
- Methods;
- Results;
- Conclusions.

These subheadings should appear in the text of the abstract and the abstract should not contain references. The abstract should: indicate the specific objective or purpose of the article; describe the methods used to achieve the objective, stating what was done and how it was done; present the findings of the methods described – key statistics should be included; present the conclusion of the study based solely on the data provided, and highlight the novelty of the work.

Beneath the abstract please select up to 5 keywords from the current Medical Subject Headings (MeSH).

Main text

Please organise your paper in a logical structure with clear subheadings to indicate relevant sections. It is up to the authors to decide the specific nature of any subheadings as they see fit. Research papers typically follow the structure:

- Introductory section;
- Methods and materials/patients;
- Results;
- Discussion;
- Conclusion;
- Acknowledgments (if relevant).

Present results in a clear logical sequence. The conclusions drawn should be supported by the results obtained and the discussion section should comment critically on the findings and conclusions as well as any limitations of the work.

Acknowledgments should be brief and should indicate any potential conflicts of interest and sources of financial support.

An appendix may be used for mathematical formulae or method details of interest to readers with specialist knowledge of the area.

In addition:

- Avoid repetition between sections.
- Avoid repetition of text featured in tables and the main body of the article.
- Abbreviations and acronyms may be used where appropriate, but must always be defined where first used.
- The names and locations (town, country) of manufacturers of all equipment and non-generic drugs must be given.
- Avoid the use of footnotes.
- Use SI units throughout the text (Grays, Sieverts not RADs and REMs).

References

- Authors are responsible for the accuracy of the references. Only papers closely related to the work should be cited; exhaustive lists should be avoided. All references must appear both in the text and the reference list.
- References should follow the Vancouver format.
- In the text, references are cited in numerical order as superscript numbers starting at 1. The superscript numbers are placed AFTER the full point.
- At the end of the paper they should be listed (double-spaced) in numerical order corresponding to the order of citation in the text.
- A reference cited in a table or figure caption counts as being cited where the table or figure is first mentioned in the text.
- Papers in press may be included in the list of references.
- Do not include references to uncompleted work or work that has not yet been accepted for publication. Abstracts and/or papers presented at meetings not in the public domain should not be included as references.
- References to private communications should be given only in the text (i.e. no number allocated). The author and year should be provided.
- If there are 6 or fewer authors, list them all. If there are 7 or more, list the first 6 followed by et al.
- Abbreviations for titles of medical periodicals should conform to those used in the latest edition of Index Medicus.
- The first and last page numbers for each reference should be provided.
- Abstracts and letters must be identified as such.

Examples of references:

Journal article:
Gardner DG, Kessler HP, Morency R, Schaffner DL. The glandular odontogenic cyst: an apparent entity. J Oral Pathol 1988; 17:359–366.

Journal article, in press:
Dufoo S, Maupome G, Diez-de-Bonilla J. Caries experience in a selected patient population in Mexico City. Community Dent Oral Epidemiol (in press).

Complete book:
Kramer IRH, Pindborg JJ, Shear M. Histological typing of odontogenic tumours (2nd edn). Berlin: Springer Verlag, 1992.

Chapter in book:
DelBalso AM, Ellis GE, Hartman KS, Langlais RP. Diagnostic imaging of the salivary glands and periglandular regions. In: DelBaso AM (ed). Maxillofacial imaging. Philadelphia, PA: WB Saunders, 1990, pp 409–510.

Abstract:
Mileman PA, Espelid I. Radiographic treatment decisions - a comparison between Dutch and Norwegian practitioners. J Dent Res 1986; 65: 609 (Abstr 32).

Letter to the Editor:
Gomez RS, de Oliveira JR, Castro WH. Spontaneous regression of a paradental cyst. Dentomaxillofac Radiol 2001; 30: 296 (letter).

Journal article on the internet:
Abood S. Quality improvement initiative in nursing homes: the ANA acts in an advisory role. Am J Nurs [serial on the Internet]. 2002 Jun [cited 2002 Aug 12];102(6):[about 3 p.]. Available from: http://www.nursingworld.org/AJN/2002/june/Wawatch.htm.

Homepage/Web site:
Cancer-Pain.org [homepage on the Internet]. New York: Association of Cancer Online Resources, Inc.; c2000-01 [updated 2002 May 16; cited 2002 Jul 9]. Available from: http://www.cancer-pain.org/.

Tables

Tables should be referred to specifically in the text of the paper but provided as separate files.

- Number tables consecutively with Arabic numerals (1, 2, 3, etc.), in the order in which they appear in the text.
- Give each table a short descriptive title.
- Make tables self-explanatory and do not duplicate data given in the text or figures.
- Aim for maximum clarity when arranging data in tables. Where practicable, confine entries in tables to one line (row) in the table, e.g. "value (±sd) (range)" on a single line is preferred to stacking each entry on three separate lines.
- Ensure that all columns and rows are properly aligned.
- Include horizontal rules at the top and bottom of a table and one below the column headings. If a column heading encompasses two or more subheadings, then the main headings and subheadings should be separated by a single short rule. No other rules should be included, neither horizontal nor vertical.
- Appropriate space should be used to separate columns. Rows should be double-spaced.
- A table may have footnotes if necessary. These should be referred to within the table by superscript letters, which will then also be given at the beginning of the relevant footnote. Begin each footnote on a new line. A general footnote referring to the whole table does not require a superscript letter.
- Define abbreviations in tables in the footnotes even if defined in the text or a previous table.
- Submit tables as editable text.

Figures

Figures should be referred to specifically in the text of the paper.

- Number figures consecutively using Arabic numerals (1, 2, 3, etc.) and any figure that has multiple parts should be labelled alphabetically (e.g. 2a, 2b).
- Concise, numbered legend(s) should be listed on a separate sheet. Avoid repeating material from the text.
- Abbreviations used in figures should be defined in the caption.
- Labelling of artwork should be Arial 8 point font.
- Ideally, figure sizes should be 84 mm wide, 175 mm wide or the intermediate width of 130 mm.

Files

- Supply image files in EPS, TIFF, PDF or JPEG format.
- TIFF is preferred for halftones, i.e. medical images such as radiographs, MR scans etc.
- EPS is preferred for drawn artwork (line drawings and graphs).
- For JPEG files, it is essential to save at maximum quality, i.e. "10", to ensure that quality is satisfactory when the files are eventually decompressed.
- Files supplied in Word, PowerPoint or Excel may prove acceptable, but please supply in EPS, TIFF or JPEG if practicable. Other formats will not be usable.
- Do not supply GIF files – GIF is a compressed format that can cause quality problems when printed.
- Upload each figure separately and numbered.

Colour

- Unless essential to the content of the article, all illustrations should be supplied in black and white with no colour (RGB, CMYK or Pantone references) contained within them.
- The cost of reproduction of colour images will be charged to the author at the following rates: £300 for one colour image, £500 for two colour images and £100 for each subsequent additional colour image. All prices are exclusive of UK VAT.
- Images that do need to be reproduced in colour should be saved in CMYK, with no RGB or Pantone references contained within them.

Resolution

- Files should be saved at the appropriate dpi (dots per inch) for the type of graphic (the typical screen value of 72 dpi will not yield satisfactory printed results). Lower resolutions will not be usable.
- Line drawings – save at 800 dpi (or 1200 dpi for fine line work).
- Halftone and colour work – save at 300 dpi.

Composition

- The image should be cropped to show just the relevant area (i.e. no more than is necessary to illustrate the points made by the author whilst retaining sufficient anatomical landmarks). The amount of white space around the illustration should be kept to a minimum.
- Supply illustrations at the size they are to be printed, usually 76 mm wide (single column of text) or for especially large figures 161 mm (two columns of text).
- Annotations, e.g. arrows, should be used to indicate subtle but salient points. All annotations should be included within the images supplied.
- Patient identification must be obscured.

Additional points to note:

- Do not put a box around graphs, diagrams or other artwork.
- Avoid background gridlines unless these are essential (e.g. confidence limits).
- Fonts should be Adobe Type 1 standard – Helvetica or Times are preferred.
- Ensure that lettering is appropriately sized – should correspond to 8 or 9 pt when printed.
- Include all units of measurement on axes.
- All lines (e.g. graph axes) should have a minimum width of ¼ pt (0.1 mm) otherwise they will not print; 1 pt weight is preferable.
- Avoid using tints (solid black and white or variations of crosshatching are preferred), but any tints that are used must be at a minimum 5% level to print (but do not use too high a tint as it may print too dark).
- Do not use three-dimensional histograms when the addition of a third dimension gives no further information.

Appendices

Appendices should be used to include detailed background material that is essential for the understanding of the manuscript e.g. statistical analyses, very detailed preliminary studies, but which is too comprehensive to include as part of the main text.

Where possible, authors are encouraged to include all relevant material in the main body of the text, however, if an appendix is necessary it should be supplied as a separate file. If more than one appendix is included, these should be identified using different letters.

- An appendix may contain references, but these should be listed separately and numbered A1, A2, etc.
- Appendices must be referred to in the main text in the relevant section.

Supplementary material

Supplemental material is intended for material that would add value to your manuscript but is not essential to the understanding of the work. Supplementary material is typically used for including material that can not be accommodated in print form, for example multimedia files such as dynamic images, video/audio files etc.

There are no restrictions on supplementary file formats, though it is recommended that authors choose file types that the majority of readers will be able to open e.g.

- Text/Data: PDF, Word, Excel, Powerpoint, .txt
- Graphics: TIF, PNG, JPEG, GIF
- Video: AVI, MOV, MP4, MPEG, WMV
- Audio: mp3, m4a

Units, symbols and statistics

Authors should use the International System of Units (SI) [1]. Units of radiation should be given in SI, e.g. 1 Sv, 1 Gy, 1 MBq. Exceptions are mmHg for blood pressure and g dl–1 for haemoglobin. For guidance, authors can refer to the publication Units, Symbols and Abbreviations. A guide for medical and scientific authors [2].

- All radiation factors (dose/time/fractionation) must be listed.
- Equations should be numbered (1), (2) etc. to the right of the equation. Do not use punctuation after equations.
- Do not include dots to signify multiplication – parameters should simply be typed closed up, or with a multiplication sign if necessary to avoid ambiguity.

Statistical Guidelines

The aim of the study should be clearly described and a suitable design, incorporating an appropriate number of subjects, should be used to accomplish the aim. It is frequently beneficial to consult a professional statistician before undertaking a study to confirm it has adequate power, and presentation of a power calculation within the paper demonstrates the ability of the study to detect clinically or biologically meaningful effects.

Details should be provided on selection criteria, whether data were collected prospectively or retrospectively, and any exclusions or losses to follow-up that might affect the study population. Information on subject characteristics in groups being compared should be given for any factors that could potentially bias the comparison of the groups; such information is often best presented in a tabular format in which the groups are in adjacent columns. If the study was randomized, details of the randomization procedure should be included.

Measures of variation should be included for all important results. When means are presented, the standard deviation or the standard error of the mean should also be given, and it should be clear which of these two measures is being quoted. When medians are given, measures of variation such as the interquartile range or overall range should also be included. Estimates of differences, e.g. between two means being compared, should be provided with 95% confidence limits to aid the reader and author to interpret the results correctly. Note that estimation of the size of effects, e.g. treatment or prognostic factor effects, is as important as hypothesis testing.

Statistical procedures should be described and referenced for all p-values given, and the values from which they were derived should be included. The validity of statistical procedures should also be confirmed, e.g. the t-test requires normal distribution(s) in the basic data and the chi-squared test is not valid when the expected numbers in cells are less than 5. Data may sometimes be transformed, e.g. using a log or square root transformation, to achieve normality. Non-parametric tests should be used when the conditions for normality are not met. It should be noted, however, that the Wilcoxon signed rank test (the non-parametric equivalent of the paired t-test) is semi-quantitative. If more than two groups are being compared then an analysis of variance should be performed before undertaking comparisons of pairs of groups. You are advised to seek the help of a professional statistician if you are uncertain of the appropriateness or interpretation of statistical methods.

Analysis of repeated measurements on the same subject can give rise to spurious results if comparisons are made at a large number of different time points. It is frequently preferable to represent each subject's outcome by a single summary measure chosen for its appropriateness. Examples of such measures are the area under the curve, the overall mean, the maximum or minimum, and the time to reach a given value. Simple statistics can then be applied to these summary measures.

The results of the evaluation of a test procedure should state clearly the criteria used to define positivity, and the sensitivity, specificity, positive predictive value and negative predictive value should all be quoted together with their 95% confidence limits.

1. Goldman DT, Bell RJ, eds. The International System of Units (SI). 5th edn. London, UK: HMSO; 1987.

2. Baron DN, ed. Units, symbols and abbreviations. A guide for medical and scientific authors. 5th edn. London, UK: Royal Society of Medicine Press; 1994.

ANEXO B – Comprovante de Submissão

Data:27/06/2018 21:01
De:"DMFR Office" <em@editorialmanager.com>
Para:"Karina Lopes Devito" <karina.devito@ufjf.edu.br>
Responder para:"DMFR Office" <rschulze@uni-mainz.de>

Dear Karina Devito,

You are receiving this e-mail as you are listed as the corresponding author or as a co-author on the submission entitled "Quantification of metallic artifacts produced by dental implants in CBCT images obtained using different acquisition protocols", which has been received by Dentomaxillofacial Radiology.

You will be able to check on the progress of your paper by logging on to Editorial Manager as an Author at https://dmfr.editorialmanager.com/.

If you already know your password, please login with it. If you have just been registered, or you have forgotten your password, please activate the following link to create a password: https://dmfr.editorialmanager.com/l.asp?i=35534&l=ZOVYOZI3. If you cannot activate the above password link please go to "https://dmfr.editorialmanager.com/", click "login" then click "Send login details" or please notify me by replying directly to this email.

You will be informed by email of the manuscript reference number in due course.

If you do not think you should be listed as an author of this work, please get in touch with the editor (rschulze@uni-mainz.de)

Thank you for submitting your work to DMFR.

Kind regards,
DMFR Office